

Influence of Similarity Law on Movement Characteristics of Vibration Actuator

Hiroyuki Yaguchi¹ & Yusuke Itoh¹

¹ Faculty of Engineering, Tohoku Gakuin University, Miyagi, Japan

Correspondence: Hiroyuki Yaguchi, Faculty of Engineering, Tohoku Gakuin University, 1-13-1 Chuo, Tagajo, Miyagi, Japan. Tel: 81-22-368-7104. E-mail: yaguchi@mail.tohoku-gakuin.ac.jp

Received: May 29, 2018

Accepted: July 16, 2018

Online Published: July 27, 2018

doi:10.5539/mer.v8n2p1

URL: <https://doi.org/10.5539/mer.v8n2p1>

Abstract

Currently, a belt conveyor or an automatic guided vehicle is used as a conveying device in a factory. However, Transportation of the ceiling surface and the wall surface in these devices is impossible. Elevator is used for conveying from the lower floor to the upper floor. Therefore, the conveying device capable of movement on a wall and a ceiling significantly improves the efficiency of work. Based on this background, development of working robots capable of transporting on a wall surface is required. In the present study, the vibration actuator with a very simple structure capable of movement on a magnetic substance by means of the inertial force of a vibration model was again considered. Furthermore, upsizing for the actuator in order to improve the propulsion characteristics was considered. The volume of the permanent magnet constituting the vibration component of the actuator was increased according to the similarity rule. Four models of actuator with approximately equal drive frequency were prototyped and experimentally tested. The experimental results demonstrate that the maximum efficiency of the actuator for a standard model pulling its own weight was 27.1 %. Furthermore, the actuator is able to pull a load mass of 170 g. For the actuator of 5 times model, the actuator is able to climb upward at 9.5 mm/s while pulling a load mass of 3500 g. This actuator is able to propel a load mass of approximately 36 times the weight of the actuator itself.

Keywords: vibration actuator, wall climbing, similarity law, propulsion performance, efficiency

1. Introduction

Currently, a belt conveyor or an automatic guided vehicle is used as a conveying device in a factory. However, Transportation of the ceiling surface and the wall surface in these devices is impossible. Elevator is used for conveying from the lower floor to the upper floor. Therefore, the conveying device capable of movement on a wall and a ceiling significantly improves the efficiency of work. On the other hand, in the construction site, cranes for the site are used for lifting and lowering of heavy weight goods. Due to the simple rail installation, the transport system capable of movement with respect to heavy goods considerably improves efficiency of work. Based on this background, development of working robots capable of transporting on a wall surface is required.

A number of studies have investigated the mechanisms of a robot capable of climbing the vertical surfaces. Adsorption methods for wall surface movement have used the following proposed techniques: by using the magnetic circuit that the magnetic pole of the permanent magnet was placed in turn, type that these were inserted in a caterpillar (Shen et al., 2011; Lee et al., 2011), type using an absorption force of a sucker manufactured with a sponge (Kawasaki et al., 2014) or flexible rubber (Yoshida et al., 2011; Suzuki et al., 2010), type capable of movement on an iron plate by controlling an attractive force of an electromagnet inserted in a robot (Khiradeet al., 2014), type capable of movement on an iron plate by combination a permanent magnet and an iron wheel (Kim et al., 2010; Kim et al., 2008), type to adsorb by producing negative pressure using a pump (Subramanyam et al., 2011; Jae et al., 2013), by vibrating many caps of the sucker (Wang et al., 2008; Wang et al., 2010), type capable of movement on the rough surface such as the concrete using a claw gripper (Xu et al., 2012; Funatsu et al., 2014), type capable of movement on a wall surface using adhesive material (Provancher et al., 2011; Kute et al., 2010; Unver et al., 2009).

Mobile robots capable of wall climbing generally move at low speeds because of problems with controllability and their high weight resulting. A lightweight actuator and with superior operability is expected in the inspection field. A novel vibration actuator capable of movement on a magnetic substance by coupled an electromagnetic force and a mechanical vibration has been proposed (Yaguchi et al., 2015; Yaguchi et al., 2016; Yaguchi et al., 2017) by authors. This vibration has very simple structure. Furthermore, direct drive is possible without a link mechanism and

reduction gear mechanism because this actuator has high promotion properties. In addition, the actuator is capable of both slide-on-ceiling and wall-climbing motions. However, since this vibration actuator is very small, it is impossible to carry heavy goods.

In the present study, the vibration actuator with a very simple structure capable of movement on a magnetic substance by means of the inertial force of a vibration model was again considered. Furthermore, upsizing for the actuator in order to improve the propulsion characteristics was considered. The volume of the permanent magnet constituting the vibration component of the actuator was increased according to the similarity rule. The actuator with the volume of the permanent magnet used in the previous study (Yaguchi et al., 2017) was used as a standard model, and the actuator with permanent magnet volume of 2 times, 3 times and 5 times for the standard model is trial manufactured, respectively. Four models of actuators with approximately equal drive frequency were prototyped and experimentally tested.

The experimental results demonstrate that the maximum efficiency of the actuator for the standard model pulling its own weight was 27.1 %. Furthermore, the actuator is able to pull a load mass of 170 g. For the actuator of 2 times model, this actuator is able to climb upward at 9.1 mm/s while pulling a load mass of 850 g when input power was 1.4 W. For 5 times model, the actuator is able to climb upward at 9.5 mm/s while pulling a load mass of 3500 g. This actuator is able to propel a load mass of approximately 36 times the weight of the actuator itself. The actuator was confirmed to be able to move on magnetic substances, such as iron rails, powered by only a function generator and a power amplifier.

2. Structure of Vibration Actuator

Figure 1 shows an outline of the vibration actuator capable of movement on a magnetic substancesuch as an iron rail, as developed in a previous paper (Yaguchi et al., 2017). The vibration actuator consists of a permanent magnet, a translational spring, an electromagnet, a triangular acrylic frame, and a rubber permanent magnet attached to the bottom of the frame. The permanent magnet is a cylindrical NdFeB and is magnetized in the axial direction. Its dimensions are 12 mm in diameter and 5 mm in height. The surface magnetic flux density measured using a teslameter was 358 mT. The translational spring is a stainless steel compression coil with an outer diameter of 12 mm, a free length of 25 mm, and a spring constant k of 2,178 N/m. The vibration component was constructed using a translational spring and a cylindrical permanent magnet. The electromagnet was inserted into the translational spring. The vibration component was inclined at an angle of 60 degrees from the horizontal plane. The rubber permanent magnet was attached to the bottom of the triangular frame, which was magnetized in the thickness direction. This rubber magnet has a length of 10 mm, a width of 15 mm, and a thickness of 3 mm. The average surface magnetic flux density measured using a teslameter was 110 mT. An electromagnet with an iron core of 3.5 mm in diameter and 22 mm in length with 790 turns of 0.2-mm copper wire was used in the experiment. The iron core of the same size electromagnet was used, and a basic model of the actuator was prototyped. The first prototyped actuator was based on the previous result that the dimensions of the electromagnet were optimized. As compared with the previous study (Yaguchi et al., 2017), the number of coil turns was increased by about 1.5 times from 540 turns to 790 turns. The actuator has a height of 40 mm, a width of 15 mm, and a total mass of 14.5 g.

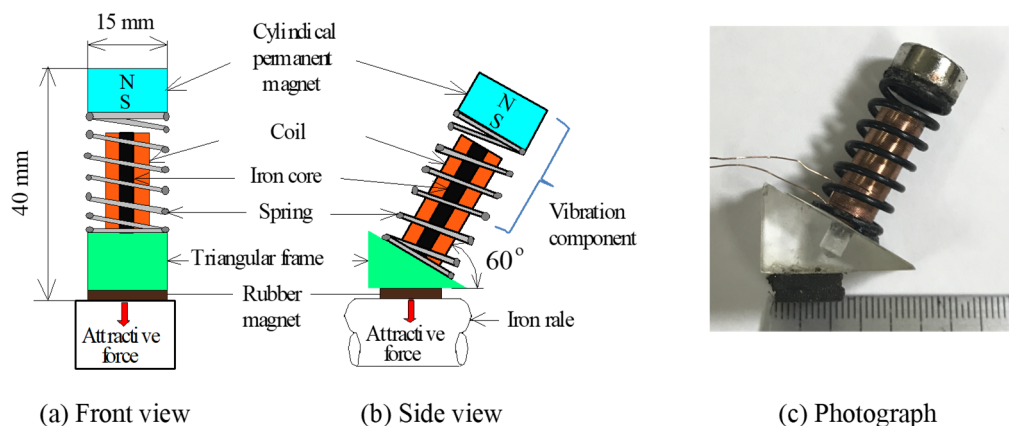


Figure 1. Structure for vibration actuator of standard model

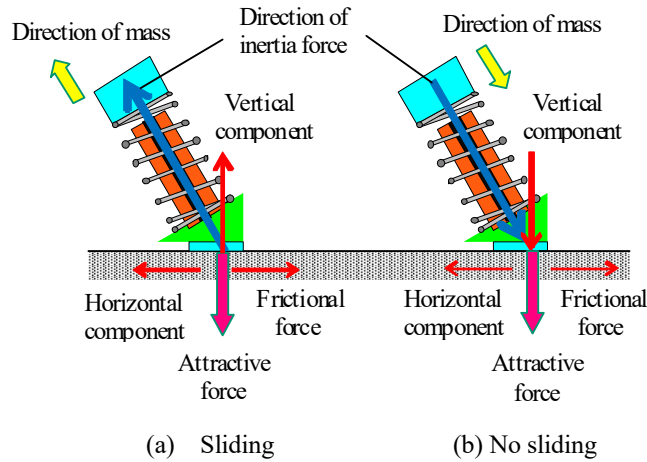


Figure 2. Principle of locomotion

The attractive force generated by a flexible magnet attached at the support acts on the actuator when this magnetic actuator is placed on a magnetic substance as shown in Figure 2. Accordingly, this actuator is able to vibrate. The frictional force between the flexible magnet and the magnetic substance alternates during one period of vibration. Due to the horizontal component of the inertial force exceeding the frictional force, the actuator is able to slide only in one direction. Thus, the magnetic actuator is propelled by the difference in frictional force between the forward and backward motions as shown in previous study.

3. Locomotion Characteristics of Vibration Actuator for Standard Model

In experiment, the iron rail with a width of 50 mm, a thickness of 50 mm, and a length of 400 mm was used. The vibration component was driven at the resonance frequency of 102 Hz using a function signal generator and an amplifier. During the measurement, the coefficient of friction was 0.7. An experimental test was conducted using the apparatus shown in Figure 3. The attractive force was measured by attracting the actuator to the iron rail and pulling the actuator body by using a spring balance. This actuator is capable of both slide-on-ceiling and wall-climbing motions. In this paper, in order to evaluate the propulsion performance, the speed of the actuator was measured specializing in the vertical upward.

Figure 4 shows the relationship between the load mass and the speed of the upward movement for input powers of 0.08, 0.13, and 0.24 W when the attractive force by the rubber magnet was 2.3 N. The load was attached to the actuator with a string. This figure shows that the actuator was able to climb upward at 36 mm/s while pulling a load of 110 g when the input power was 0.24 W.

The solid lines in Figure 5 show the relationship between the load mass and the efficiency including own-weight of the vibration actuator when the attractive force by the rubber magnet was 2.3 N. The input power of the electromagnet was set to 0.08, 0.13, and 0.24 W. The efficiency η is expressed as

$$\eta [\%] = (M_a + M_m) v_{up} G \times 100 / P_1 \quad (1)$$

where M_a is the total mass of the actuator, M_m is the mass of the load, v_{up} is the vertical upward speed, G is the acceleration due to gravity, and P_1 is the input power. The maximum efficiency of the actuator was 27.1 % for the case with own-weight to calculate self-propellant efficiency. Due to increasing the number of turns for the electromagnet of about 1.5 times, the maximum efficiency improved from 15 % of the previous study to 27 %.

On the other hand, Figure 6 shows the relationship between the load mass and the speed of the upward movement for input powers of 0.08, 0.13, and 0.24 W when the attractive force by the rubber magnet was 3 N. The solid lines in Figure 7 show the relationship between the load mass and the efficiency including own-weight of the vibration actuator when the attractive force by the rubber magnet was 3 N. The input power of the electromagnet was set to 0.08, 0.13, and 0.24 W.

Considering Figure 4 to Figure 7, the movement characteristics of the actuator change considerably as the attractive force changes. When the attractive force is small, it demonstrates high speed and low propulsion type characteristics. On the other hand, when the attractive force is large, the movement characteristic is a high propulsion type at low

speed. Thus, by changing the attractive force of the actuator, the propulsion characteristics change dramatically. Due to the reason that the propulsion property depends on the attractive force, it is necessary to increase the attractive force for carrying heavy loads. When the attractive force is large, the amplitude of the vibration component increases and high propulsion performance is provided. However, since frictional losses between the rubber magnet and the iron rail also increase drastically, the efficiency of the actuator decreases considerably.

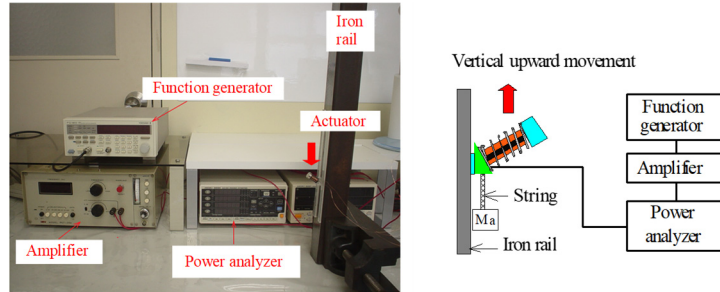


Figure 3. Experimental apparatus and vibration actuator

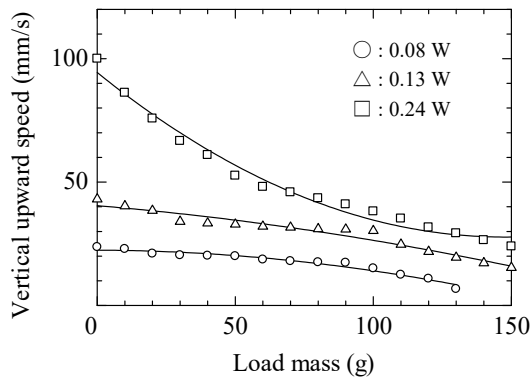


Figure 4. Relationship between load mass and vertical upward speed (Standard model, attractive force 2.3 N)

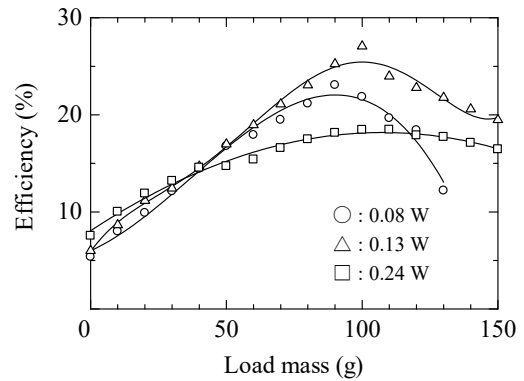


Figure 5. Relationship between load mass and efficiency (Standard model, attractive force 2.3 N)

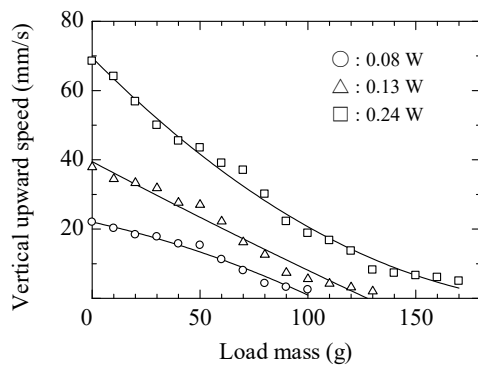


Figure 6. Relationship between load mass and vertical upward speed (Standard model, attractive force 3 N)

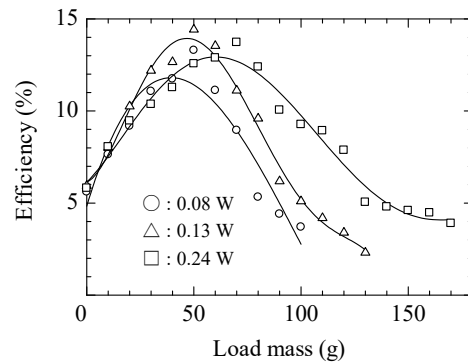


Figure 7. Relationship between load mass and efficiency (Standard model, attractive force 3 N)

4. Upsizing of the Actuator by the Similarity Rule and Locomotion Characteristic

Furthermore, examination to increase the size of the actuator in order to improve the propulsion characteristics was carried out. As a method of upsizing, the volume of the permanent magnet constituting the vibration component was increased according to the similarity rule. The permanent magnet of the actuator demonstrated in the previous section is used as the standard model (1 time), and actuators with prototype permanent magnet volume of 2 times, 3 times and 5 times model in the standard model were prototyped. The height of the permanent magnet was unified to

about 5 mm. In this actuator, the movement speed is proportional to the driving frequency. The spring constant of the coil spring was selected so that the resonance frequency for each actuator was about 100 Hz. The iron core volume of the electromagnet was increased 2 times, 3 times and 5 times compared to the standard model. The specifications of springs, permanent magnets, electromagnets of each model are shown in Table 1.

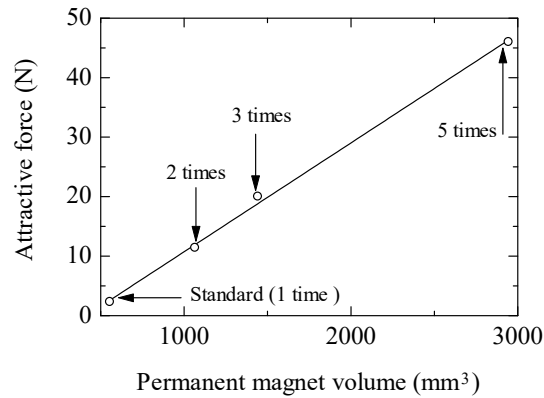
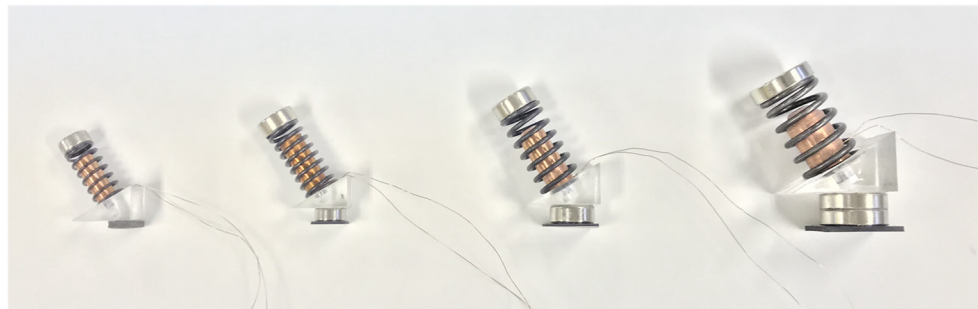


Figure 8. Relationship between magnet volume and attractive force.

Table 1. Specification for each prototype actuator

Type of actuator		Standard (1 time)	2 times	3 times	5times
Coil spring	Diameter (mm)	12	15	17.5	25
	Height (mm)	5	6	6	6
	Free length (mm)	25	30	35	35
	Outer diameter (mm)	11	14	18	24
	Spring constant (N/mm)	2.178	4.812	6.38	10.161
Electromagnet	Diameter of iron core (mm)	7.6	8.7	11.4	20.7
	Length of iron core (mm)	22	23	23	23
	Number of turns	790	1200	1800	2200



(a) Standard model (b) 2 times model (c) 3 times model (d) 5 times model

Figure 9. Photograph of actuators

Table 2. Magnet volume, total mass and 1ttractive force for each actuator

Type of actuator	Standard (1 time)	2 times	3 times	5times
Volume of permanent magnet (mm ³)	556	1066	1443	2945
Magnet type and size at support	Rubber	NdFeB ($\Phi 12 \times 3$ mm)	NdFeB ($\Phi 17 \times 5$ mm)	NdFeB ($\Phi 25 \times 6$ mm)
Attractive force (N)	2.3	11.5	20	46
Thickness of rubber sheet (mm)	0	0.5	1	3
Total mass of actuator (g)	14.5	30.3	69.5	97.1

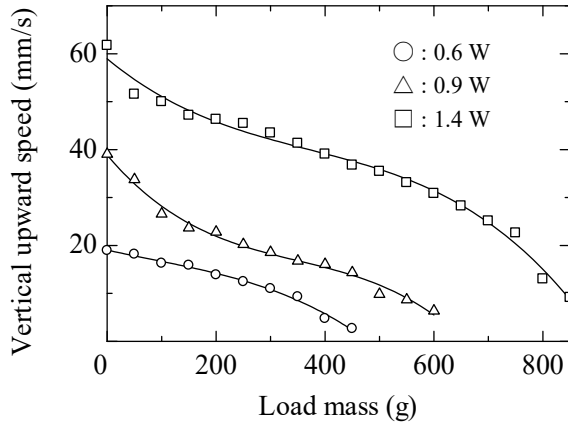


Figure 10. Relationship between load mass and vertical upward speed (2 times model, attractive force 11.5 N)

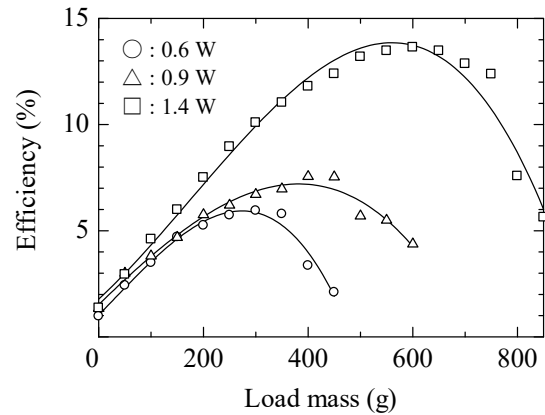


Figure 11. Relationship between load mass and efficiency (2 times model, attractive force 11.5 N)

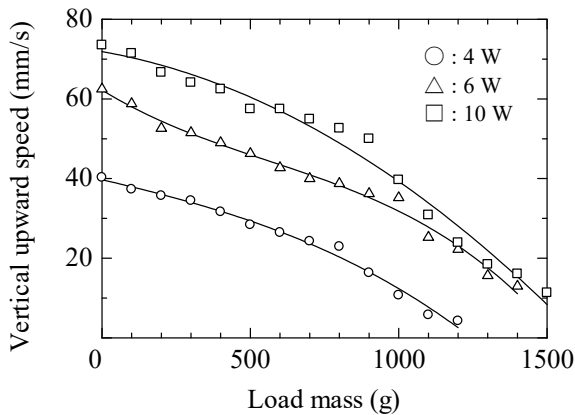


Figure 12. Relationship between load mass and vertical upward speed (3 times model, attractive force 20 N)

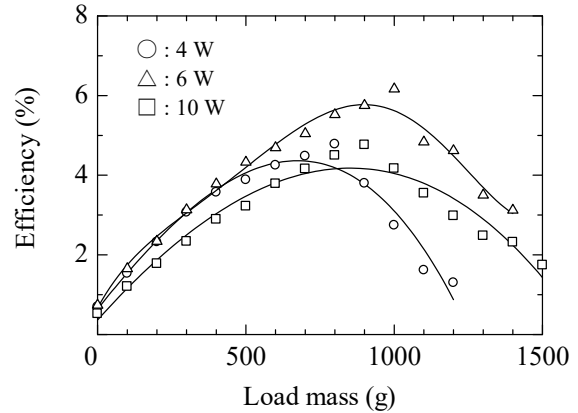


Figure 13. Relationship between load mass and efficiency (3 times model, attractive force 20 N)

As mentioned in the previous chapter, selection of the attractive force is very important. The attractive force for each model was selected to be linearly proportional to the permanent magnet volume as shown in Figure 8. For the standard model, the rubber permanent magnet was used at the support part of the actuator. In each model, the support part combines the NdFeB permanent magnet and a thin natural rubber sheet, respectively. The photographs of each actuator are shown in Figure 9. Table 2 shows the volume of permanent magnet, NdFeB permanent magnet used at the support part, the attractive force, the natural rubber sheet and total mass of the in each actuator. In addition, 0.2-mm copper wire for each model was used for the electromagnet.

For 2 times mode, the actuator has a height of 47 mm, a width of 15 mm, and a total mass of 30.3 g. Figure 10 shows the relationship between the load mass for the actuator of 2 times model and the speed of the upward movement for input powers of 0.6, 0.9, and 1.4 W when the attractive force by the NdFeB magnet was 11.5 N. The figure indicates that the actuator is able to climb upward at 10 mm/s while pulling a load mass of 850 g when input power was 1.4 W. This actuator is able to propel a load mass of approximately 28 times the weight of the actuator itself. With increase in load mass, the vertical upward speed of the actuator decreases approximately linearly. Even if the load mass exceeding 850 g is loaded on the actuator, this actuator was not able to move. This is the limit value of the propulsion performance by the attraction force of the actuator.

Figure 11 shows the relationship between the load mass for the actuator of 2 times model and the efficiency including own-weight of the actuator when the attractive force by the NdFeB magnet was 11.5 N. The input power of the electromagnet was set to 0.08, 0.13, and 0.24 W. Each curve of the efficiency shows the maximum value, respectively. The maximum efficiency of the actuator was 14 % for the case with own-weight when input power was 1.4 W. There is an optimum input power that maximizes the efficiency of the actuator.

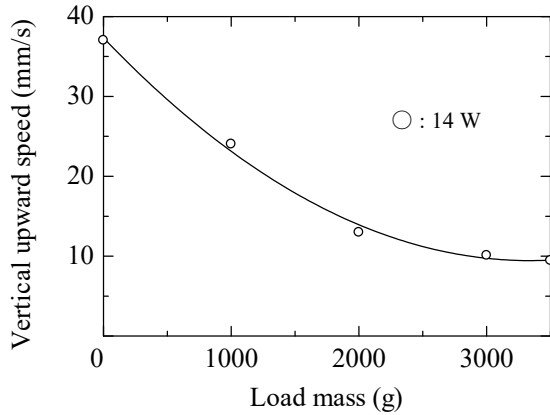


Figure 14. Relationship between load mass and vertical upward speed (5 times model, attractive force 46 N)

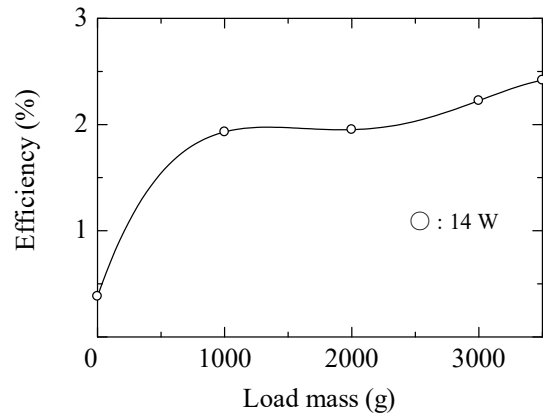


Figure 15. Relationship between load mass and efficiency (5 times model, attractive force 46 N)

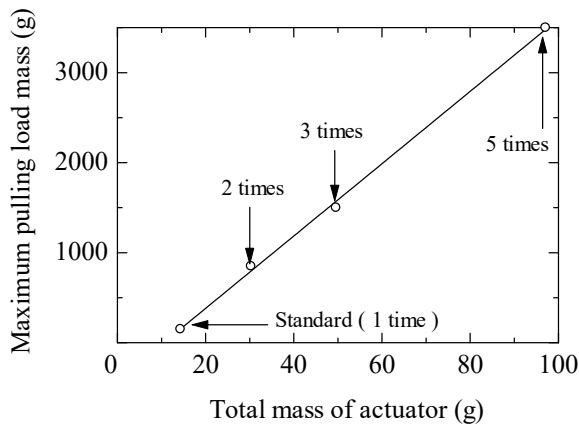


Figure 16. Relationship between total mass of actuator and maximum pulling load mass

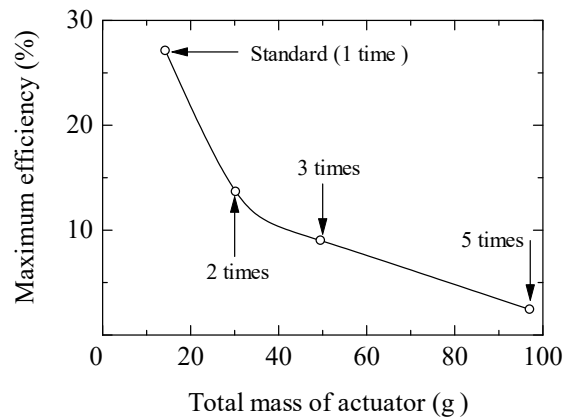


Figure 17. Relationship between total mass of actuator and maximum efficiency

For 3 times mode, the actuator has a height of 56 mm, a width of 20 mm, and a total mass of 69.5 g. Figure 12 shows the relationship between the load mass for the actuator of 3 times model and the speed of the upward movement for input powers of 4 W, 6 W and 10 W when the attractive force by the the NdFeB magnet was 20 N. The figure indicates that the actuator is able to climb upward at 10 mm/s while pulling a load mass of 1500 g when input power was 10 W. This actuator is able to propel a load mass of approximately 30 times the weight of the actuator itself. Figure 13 shows the relationship between the load mass and the efficiency including own-weight of the actuator when the attractive force by the the NdFeB magnet was 20 N. The input power of the electromagnet was set to 4 W, 6 W and 10 W. The maximum efficiency of the actuator was 6 % when input power was 6 W.

For 5 times mode, the actuator has a height of 65 mm, a width of 30 mm, and a total mass of 97.1 g.

Figure 14 shows the relationship between the load mass for the actuator of 5 times model and the speed of the upward movement for input powers of 14 W when the attractive force by the the NdFeB magnet was 46 N. The figure indicates that the actuator is able to climb upward at 10 mm/s while pulling a load mass of 3500 g. This actuator is able to propel a load mass of approximately 36 times the weight of the actuator itself. The movement speed of the actuator at no load mass is 37.4 mm/s because the suction force is very high. An adhesive was used to make this actuator. When power exceeding 14 W was input to the actuator, the adhesion was peeled off. In the future, a welding process is required for making actuator. Figure 15 shows the relationship between the load mass and the efficiency including own-weight of the actuator when the attractive force by the the NdFeB magnet was 46 N. The input power of the electromagnet was set to 14 W. The maximum efficiency of the actuator was 2.4 %.

The results obtained from experiments were summarized. Figure 16 shows the relationship between the total mass m (g) of each actuator and maximum pulling load mass M (g). The maximum pulling load mass increases linearly as the total mass of the actuator increases. From these results, the following linear equation is obtained.

$$M \text{ (g)} = -421.8 + 40.18 m \text{ (g)} \quad (2)$$

From the above equation, the maximum pulling force is about 400 N when the total mass of the actuator is 1 kg. Further, when the total mass of the actuator is 5 kg, the maximum traction force becomes 2000 N. It is expected that the pulling force of 40 times compared to its own weight can be generated. Since a reduction gear such as a gear is not required, it is possible to realize a compact and high propulsive conveying device.

Figure 17 shows the relationship between the total mass m of each actuator and maximum efficiency. The maximum efficiency decreases curvilinearly as the mass increases. When the actuator becomes large, it is necessary to increase the attractive force. Therefore, the increase in friction loss is the reason for the decrease in efficiency. We need to improve the magnetic circuit and change the structure and improve the efficiency. In addition, when a heavy load is mounted on the actuator, since the movement speed is low as the conveying device, consideration to increase the speed is necessary.

5. Conclusion

A novel vibration actuator capable of movement by means of an inertial force has been proposed. Upsizing for the actuator in order to improve the propulsion characteristics was considered. The volume of the permanent magnet constituting the vibration component of the actuator was increased according to the similarity rule. Four models of actuator with approximately equal drive frequency were prototyped and experimentally tested.

The experimental results demonstrate that the maximum efficiency of the actuator for the standard model pulling its own weight was 27.1 %. Furthermore, the actuator is able to pull a load mass of 170 g. For the actuator of 3 times model, this actuator is able to climb upward at 9.1 mm/s while pulling a load mass of 1450 g when input power was 10 W. For 5 times model, the actuator is able to climb upward at 9.5 mm/s while pulling a load mass of 3500 g. This actuator is able to propel a load mass of approximately 36 times the weight of the actuator itself. The results obtained from experiments were summarized. Therefore, when the total mass of the actuator is 5 kg, the maximum traction force becomes 2000 N.

It is expected that the pulling force of 40 times compared to its own weight can be generated. However, when the actuator becomes large, it is necessary to increase the attractive force. Therefore, the increase in friction loss is the reason for the decrease in efficiency. In the future, we need to improve the magnetic circuit and change the structure and improve the efficiency.

References

- Funatsu, M., Kawasaki, Y., Kawasaki, S., & Kikuchi, K. (2014). Development of cm-scale Wall Climbing Hexapod Robot with Claws. *Proc., International Conference on Design Engineering and Science* (pp. 101-106).
- Jae-Uk, S., Donghoon, K., Ong-Heon, J., & Hyun, M. (2013). Micro aerial vehicle type wall-climbing robot mechanism. *Proc., IEEE RO-MAN International Symposium on Robot and Human Interactive Communication* (pp. 722-725). Retrieved from <https://ieeexplore.ieee.org/document/6628398/>.
- Kawasaki, S., & Kikuchi, K. (2014). Development of a Small Legged Wall Climbing Robot with Passive Suction Cups. *Proc., International Conference on Design engineering and science* (pp. 112-116).
- Khirade, M., Sanghi, R., & Tidke, D. (2014). Magnetic Wall Climbing Devices - A Review. *Proc., International Conference on Advances in Engineering & Technology* (pp. 55-59).
- Kim, H., Kim, D., Yang, H., Lee, K., SeoK., Chang, F., & Kim, D. (2008). Development of a wall-climbing robot using a tracked wheel mechanism, *Journal of Mechanical Science and Technology*, 22, 1490-1498. Retrieved from <https://link.springer.com/article/10.1007/s12206-008-0413-x>
- Kim, J., Park, S., Kim J., & Lee, J. (2010). Design and Experimental Implementation of Easily Detachable Permanent Magnet Reluctance Wheel for Wall-Climbing Mobile Robot, *Journal of Magnetics*, 15(3), 128-131. Retrieved from <http://komag.org/12123012/>
- Kute, C., Murphy, M., Menguc, Y., & Sitti, M. (2010). Adhesion Recovery and Passive Peeling in a Wall Climbing Robot using Adhesives. *Proc., IEEE International Conference on Robotics and Automation* (pp. 2797-2802). Retrieved from <https://ieeexplore.ieee.org/document/5509142/>.
- Lee, G., Park, J., Kim, H., & Seo, T. W. (2011). Wall Climbing Robots with Track-wheel Mechanism. *Proc., IEEE International Conference on Machine Learning and Computing* (pp. 334-337).

- Provancher, W., Jensen-Segal, S., & Fehlberg, M. (2011). ROCR: An Energy-Efficient Dynamic Wall-Climbing Robot. *IEEE Transaction on Mechatronics*, 16(5), 897-906. Retrieved from <https://ieeexplore.ieee.org/document/5546974/>.
- Shen, W., Gu, J., & Shen, Y. (2011). Permanent Magnetic System Design for the Wall-Climbing Robot, in *Proc., IEEE International Conference on Mechatronics & Automation*, 2078-2083. Retrieved from <https://ieeexplore.ieee.org/document/1626883/>
- Subramanyam, A., Mallikarjuna, Y., Suneel, S., & Bhargava, L. (2011). Design and Development of a Climbing Robot for Several Applications, *International Journal of Advanced Computer Technology*, 3(3), 15-23. Retrieved from <http://ijact.org/volume3issue3/IJ0330018/>
- Suzuki, M., & Hirose, S. (2010). Proposal of Swarm Type WallClimbing Robot System Anchor Climber and Development of Adhering Mobile Units. *The Robotics Society of Japan*, 28(5), 614-623. Retrieved from <https://ci.nii.ac.jp/naid/130002152578/>.
- Unver, O., & Sitti, M. (2010). Tankbot: A Miniature, Peeling Based Climber on Rough and Smooth Surfaces. *Proc., IEEE International Conference on Robotics and Automation* (pp. 2282-2287). Retrieved from <https://ieeexplore.ieee.org/document/5152304/>.
- Wang, K., Wang, W., Li, D., Zong, G., Zhang, H., Zhang, J., & Deng, Z. (2008). Analysis of Two Vibrating Suction Methods. *Proc., IEEE International Conference on Robotics and Biomimetics* (pp. 1313-1319). Retrieved from <https://ieeexplore.ieee.org/document/4913190/>.
- Wang, W., Wang, K., Zhang, H., & Zhang, J. (2010). Internal Force Compensating Method for Wall-Climbing Caterpillar Robot. *Proc., IEEE International Conference on Robotics and Automation* (pp. 2816-2820). Retrieved from <https://ieeexplore.ieee.org/document/5509624/>.
- Xu, F., Wang, X., & Jiang, G. (2012). Design and Analysis of a Wall-Climbing Robot Based on a Mechanism Utilizing Hook-Like Claws, *International Journal of Advanced Robotic Systems*, 9(261), 1-12. Retrieved from <http://journals.sagepub.com/doi/full/10.5772/53895/>.
- Yaguchi, H., & Sakuma, S. (2015). A Novel Magnetic Actuator Capable of Free Movement on a Magnetic Substance. *IEEE Transaction on Magnetics*, 15(11). Retrieved from <https://ieeexplore.ieee.org/document/7150411/>.
- Yaguchi, H., & Sakuma, S. (2016). Improvement of a Magnetic Actuator Capable of Movement on a Magnetic Substance, *IEEE Transactions on Magnetics*, 52(7). Retrieved from <https://ieeexplore.ieee.org/stamp/stamp.jsp?tp=&arnumber=7419226/>.
- Yaguchi, H., & Sakuma, S. (2017). Vibration Actuator Capable of Movement on Magnetic Substance Based on New Motion Principle. *Journal of Vibroengineering*, 19(3), 1494 – 1508. Retrieved from <https://www.jvejournal.com/article/17319/>
- Yoshida, Y., & Ma, S. (2011). A Wall-Climbing Robot without any Active Suction Mechanisms. *Proc., IEEE International Conference on Robotics and Biomimetics* (pp. 2014-2019). Retrieved from <https://ieeexplore.ieee.org/document/6181587/>.

Copyrights

Copyright for this article is retained by the author(s), with first publication rights granted to the journal.

This is an open-access article distributed under the terms and conditions of the Creative Commons Attribution license (<http://creativecommons.org/licenses/by/4.0/>).